

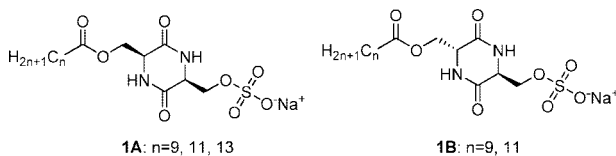
## Hydrogen-Bond-Induced Hysteresis in the Compression/Relaxation of Monolayer Films

Jennifer L. Sorrells and Fredric M. Menger\*

Department of Chemistry, Emory University, Atlanta, Georgia 30322

Received May 15, 2008; E-mail: menger@emory.edu

Morphologies of self-assemblies, like the laws of legislative assemblies, are established when opposing forces reach a compromise. For example, a micellar structure reflects a balance between attractive hydrophobic forces among internal chains and repulsive electrostatic forces among external ionic groups. Self-assembly can be affected by tinkering with either component. Over the years we have made use of this fact while synthesizing a large variety of structural modifications in amphiphilic systems. Thus, the hydrophobic region has been rigidified,<sup>1</sup> interconnected,<sup>2</sup> subdivided,<sup>3</sup> functionalized,<sup>4</sup> and hyperextended.<sup>5</sup> And the ionic surface has been provided with catalytic groups,<sup>6</sup> metals,<sup>7</sup> sugars,<sup>8</sup> macrocycles,<sup>9</sup> and zwitterions.<sup>10</sup> In the present Communication, an amphiphile has been endowed with yet another variation: a diketopiperazine ring inserted between a chain and an ionic headgroup (**1**). The question arose as to how such a ring, known to effectively hydrogen-bond with itself in linear oligomeric arrays,<sup>11</sup> perturbs the spherical assembly normally created by the hydrophobic chains. After characterizing the properties of **1** in aqueous solutions, we examined monolayer films at the air/water interface where the diketopiperazine hydrogen has a profound effect on the compression isotherms.



The synthesis of the anionic (2*S*,5*S*)-cyclo(serylserine) surfactant (**1A**) is given in Figure 1. The corresponding (2*S*,5*R*) stereoisomer (**1B**) was synthesized by a related procedure (provided in the Supporting Information). Consistent <sup>1</sup>H and <sup>13</sup>C NMR, HRMS (ESI<sup>−</sup>), and elemental analyses were obtained following multiple chromatographies on a Sephadex LH-20 size-exclusion column. An X-ray structure of the monobenzylated serine/serine diketopiperazine (Figure 2), an intermediate in the synthesis of **1B**, shows the correct relative stereochemistry plus the expected ring-to-ring hydrogen-bonding within the solid-state assembly.

Surfactants **1A** have water-solubilities of below observability for  $n = 13$ ; 0.4 mM for  $n = 11$ ; and 8 mM for  $n = 9$  (measured at 22 °C via quantitative HPLC with evaporative light scattering detection). Surfactants **1B** have water-solubilities of 0.94 mM for  $n = 11$  and 12 mM for  $n = 9$ . Since sodium dodecyl sulfate (SDS) has more than a 10-fold greater solubility than any of these values, intermolecular hydrogen-bonding of the diketopiperazines, as in Figure 2, clearly favors the solid state.

The low solubilities at 22 °C encouraged us to explore potential Krafft phenomena in our system. Below the Krafft temperature,  $T_k$ , surfactant in solution is exclusively monomeric, whereas above  $T_k$  one observes micellization and hence a much greater solubility.<sup>12</sup> Using the fact that conductivity vs temperature plots show a break at  $T_k$ , we estimated the following Krafft temperatures: **1A** ( $n =$

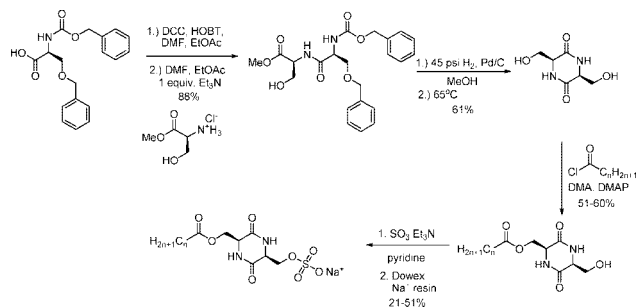
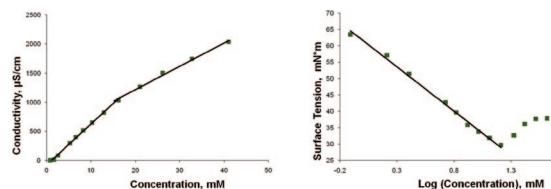
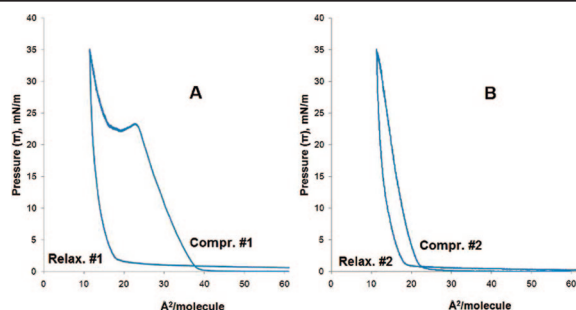
Figure 1. Synthesis of **1A**.

Figure 2. X-ray structure of monobenzyl-protected diketopiperazine made from serine. Cyclic amide-to-amide hydrogen-bonding is seen at the top of the array.

Figure 3. (Left) Conductivity vs concentration at 33 °C for **1B** ( $n = 9$ ). (Right) Surface tension vs concentration at 33 °C for **1B** ( $n = 9$ ).

11), 65–69 °C; **1A** ( $n = 9$ ), 59 °C; **1B** ( $n = 11$ ), 59 °C; **1B** ( $n = 9$ ), 27 °C. These are also the temperatures where solid suspensions could be seen to clarify. Given that short-chained anionic surfactants usually have subambient  $T_k$  values, a  $T_k$  of 59 °C for **1A** ( $n = 9$ ) is uncommonly high for a surfactant with a mere 9-carbon chain. Thus, a conventional surfactant with a 10-carbon chain, sodium decyl sulfate, has a  $T_k$  of only 9 °C.<sup>13</sup> Plots of conductivity vs concentration for **1B** ( $n = 9$ ) at ambient temperature (22 °C) are linear up to saturation, indicating an absence of micellization. When, however, the temperature was raised above the  $T_k$  to 33 °C, the plot shows an abrupt change in slope, corresponding to a critical micelle concentration (cmc) for **1B** ( $n = 9$ ) of 16 mM (Figure 3, left).

Surface tension for **1B** ( $n = 9$ ) declines linearly with the log[conc] at 22 °C, showing again that no micellization occurs below saturation at this temperature. Application of the Gibbs equation to the linear data<sup>14</sup> gave an area-per-molecule of only 40 Å<sup>2</sup>. Since this is the identical area displayed by the far less bulky SDS, one can presume that spontaneous packing at the planar air/water interface is aided by diketopiperazine hydrogen-bonding. At



**Figure 4.** (A) Compression no. 1 and relaxation no. 1 of monolayer film of **1A** ( $n = 12$ ) alcohol showing hysteresis. (B) Repeat cycle upon completion of cycle A. All subsequent cycles are identical to cycle B!

33 °C there is an abrupt change of slope at a cmc of 16 mM (the same value obtained by conductivity) (Figure 3, right). Normally, surface tension plots level off above the cmc, but in our case the slope turns positive. Although such behavior has in the past been attributed to a surface-active impurity,<sup>15</sup> quantitative NMR of our **1B** ( $n = 9$ ) sample shows that decanoic acid, if present at all, cannot exceed 0.5 wt % (an impurity level that was shown to have no effect on SDS). We believe the aberrant surface tension plot results from formation of suspended aggregates destined to become precipitated solid (an explanation consistent with a haziness that develops in the solutions just above the cmc). Thus, the picture that emerges for **1B** ( $n = 9$ ) is a rather insoluble surfactant that is monomeric at low concentrations, micellar at the cmc, and a solid phase soon thereafter. Rather than hydrophobicity and hydrogen-bonding acting in concert, they seem to play independent roles, with hydrophobicity important in micellization, and hydrogen-bonding dominating precipitation (i.e., the solid state) as the concentration is increased above the cmc.

The question remained as to the nature of the micellar phase. Since <sup>1</sup>H NMR spectra showed no significant line-broadening above the cmc, the micelles are likely small and spherical as opposed to elongated assemblies. Pulse-gradient spin-echo NMR (i.e., diffusion-NMR)<sup>16</sup> in D<sub>2</sub>O at 33 °C, coupled with the Stokes–Einstein equation, gave a hydrodynamic radius for **1B** ( $n = 9$ ) of 3.29 nm as compared with 2.45 nm for SDS. The modest increase in the diameter of **1B** ( $n = 9$ ) over SDS is likely related to the former's longer and bulkier headgroup as well as hydration of the diketopiperazine ring.

The most revealing data came from compression of monolayer films<sup>17,18</sup> of the nonsulfonated alcohol corresponding to **1A** ( $n = 11$ ). Selecting the alcohol assured that pressure/area ( $\pi/A$ ) isotherms were not perturbed by transport from the air/water interface into the aqueous subphase while the insoluble film was being compressed. Figure 4A shows a  $\pi/A$  isotherm at 20 °C in which the film was compressed at 4.0 Å<sup>2</sup>/mol/min up to 35 mN/m pressure (a value insufficient to destroy the monolayer). A transition from expanded to condensed phases is clearly visible in compression no.1. The “lift-off” area near 40 Å<sup>2</sup>/mol is twice that expected for a single-chained amphiphile, indicating that intermolecular assembly at the interface begins at a particularly low surface concentration. Even more striking is the unprecedented hysteresis seen in Figure 4A upon the relaxing the monolayer back to its original low pressure. (By way of comparison, stearic acid monolayers show only a minor 2 Å<sup>2</sup>/mol shift between compression and relaxation

cycles). Moreover, all additional compressions of the alcohol, once the first compression/relaxation sequence has been completed, now show a more normal rise at 22 Å<sup>2</sup>/mol instead of 40 Å<sup>2</sup>/mol (see Figure 4B for compression no. 2).

The hysteresis is understandable in terms of horizontal-to-vertical molecular reorientation at the air/water interface. Thus, during compression no. 1 the diketopiperazine rings hydrogen-bond to each other as they initially lie flat on the air/water interface and, thereby, occupy an unusually large area for surfactant with only a single tail. When pressures near 25 mN/m are reached, the rings flip so that they are now more-or-less perpendicular to the interface where they can also hydrogen-bond but in a much smaller space. This is a stable ring orientation that remains vertical when the monolayer is expanded during relaxation no. 1, and hence the hysteresis. Since the vertical orientation is already in place throughout compression no. 2, the first phase of the compression seen in compression no. 1 is avoided. The model implies the absence of a rapid equilibrium between the vertical and horizontal states. Rearranging film molecules by a chemist, like rearranging puzzle pieces by a child, can obviously be an engaging activity.

**Acknowledgment.** We thank Dr. Kenneth Hardcastle and Dr. Shaoxiong Wu for their assistance with the X-ray analyses and diffusion NMR, respectively. We also thank Mr. Lei Shi, Dr. Dan Lundberg, and Dr. Syed Rizvi for useful discussions and Prof. Kevin Caran and Stephanie Torcivia for use of a Nima Tech DST 9005 tensiometer. This work was supported by the National Institutes of Health.

**Supporting Information Available:** Analytical and synthetic procedures including spectroscopic data and instrumentation. This material is available free of charge via the Internet at <http://pubs.acs.org>.

## References

- (1) Menger, F. M.; Ding, J. *Angew. Chem., Int. Ed.* **1996**, *35*, 2137.
- (2) Menger, F. M.; Brocchini, S.; Chem, X. Y. *Angew. Chem., Int. Ed.* **1992**, *31*, 1492.
- (3) Menger, F. M.; Peresypkin, A. V. *J. Am. Chem. Soc.* **2001**, *123*, 5614.
- (4) Menger, F. M.; Shi, L. *J. Am. Chem. Soc.* **2006**, *128*, 9338. Menger, F. M.; Chlebowski, M. E. *Langmuir* **2005**, *21*, 2689. Menger, F. M.; Galloway, A. L. *J. Am. Chem. Soc.* **2004**, *126*, 15883.
- (5) Menger, F. M.; Yamasaki, Y. *J. Am. Chem. Soc.* **1993**, *115*, 3840.
- (6) Menger, F. M.; Whitesell, L. G. *J. Am. Chem. Soc.* **1985**, *107*, 707.
- (7) Menger, F. M.; Gan, L. H.; Johnson, E.; Durst, D. H. *J. Am. Chem. Soc.* **1987**, *109*, 2800.
- (8) Barragan, V.; Menger, F. M.; Caran, K. L.; Vidil, C.; Morère, A.; Montero, J.-L. *Chem. Commun.* **2001**, 85.
- (9) Menger, F. M.; Bian, J.; Sizova, E.; Martinson, D. E.; Sereyuk, V. A. *Org. Lett.* **2004**, *6*, 261.
- (10) Menger, F. M.; Peresypkin, A. V.; Caran, K. L.; Apkarian, R. P. *Langmuir* **2000**, *16*, 9113.
- (11) Hanabusa, K.; Matsumoto, M.; Kimura, M.; Kakeki, A.; Shirai, H. *J. Colloid Interface Sci.* **2000**, *224*, 231.
- (12) Ohta, A.; Ozawa, N.; Nakashima, S.; Asakawa, T.; Miyagishi, S. *Colloid Polym. Sci.* **2003**, *281*, 363.
- (13) Osipow, L. I. *Surface Chemistry*; Reinhold Publishing Co.: New York, 1962; p 190.
- (14) Holmberg, K.; Jönsson, B.; Kronberg, B.; Lindman, B. *Surfactants and Polymers in Aqueous Solution*, 2nd ed.; John Wiley & Sons: Chichester, England, 2002; p 251.
- (15) Lin, S. Y.; Lin, Y. Y.; Chen, E. M.; Hsu, C. T.; Kwan, C. C. *Langmuir* **1999**, *15*, 4370–4376.
- (16) Lundberg, D.; Unga, J.; Galloway, A. L.; Menger, F. M. *Langmuir* **2007**, *23*, 114534.
- (17) Menger, F. M.; Wood, M. G., Jr.; Richardson, S.; Zzhou, Q.; Elrington, A. R.; Sherrod, M. J. *J. Am. Chem. Soc.* **1988**, *110*, 6797.
- (18) Birdi, K. S. *Self-Assembly Structures of Lipids and Macromolecules at Interfaces*; Kluwer Academic/Plenum Publishers: New York, 1999.

JA803491Y